PLURIPOTENT STEM CELLS

STEM CELLS
TRANSLATIONAL MEDICINE

Stem cell-derived retinal pigment epithelium from patients with age-related macular degeneration exhibit reduced metabolism and matrix interactions

Jie Gong[1]* | Hui Cai[1]* | NYSCF Global Stem Cell Array Team[2] | Scott Noggle[2] | Daniel Paull[2] | Lawrence J. Rizzolo[1,3] | Lucian V. Del Priore[1] | Mark A. Fields[1] [ORCID]

[1]Department of Ophthalmology and Visual Science, Yale University School of Medicine, New Haven, Connecticut

[2]The New York Stem Cell Foundation (NYSCF) Research Institute, New York, New York

[3]Department of Surgery, Yale University School of Medicine, New Haven, Connecticut

Correspondence
Mark A. Fields, MPH, PhD, Department of Ophthalmology and Visual Science, Yale University School of Medicine, 300 George St., Suite 8100, New Haven, CT 06511.
Email: mark.fields@yale.edu

Funding information
Alonzo Family Fund; Research to Prevent Blindness

Abstract

Modeling age-related macular degeneration (AMD) is challenging, because it is a multifactorial disease. To focus on interactions between the retinal pigment epithelium (RPE) and Bruch's membrane, we generated RPE from AMD patients and used an altered extracellular matrix (ECM) that models aged Bruch's membrane. Induced pluripotent stem cells (iPSCs) were generated from fibroblasts isolated from AMD patients or age-matched (normal) controls. RPE derived from iPSCs were analyzed by morphology, marker expression, transepithelial electrical resistance (TER), and phagocytosis of rod photoreceptor outer segments. Cell attachment and viability was tested on nitrite-modified ECM, a typical modification of aged Bruch's membrane. DNA microarrays with hierarchical clustering and analysis of mitochondrial function were used to elucidate possible mechanisms for the observed phenotypes. Differentiated RPE displayed cell-specific morphology and markers. The TER and phagocytic capacity were similar among iPSC-derived RPE cultures. However, distinct clusters were found for the transcriptomes of AMD and control iPSC-derived RPE. AMD-derived iPSC-RPE downregulated genes responsible for metabolic-related pathways and cell attachment. AMD-derived iPSC-RPE exhibited reduced mitochondrial respiration and ability to attach and survive on nitrite-modified ECM. Cells that did attach induced the expression of complement genes. Despite reprogramming, iPSC derived from AMD patients yielded RPE with a transcriptome that is distinct from that of age-matched controls. When challenged with an AMD-like modification of Bruch's membrane, AMD-derived iPSC-RPE activated the complement immune system.

KEYWORDS

age-related macular degeneration, aging, Bruch's membrane, induced pluripotent stem cells, nonenzymatic nitration, retinal pigment epithelium

---

*Jie Gong and Hui Cai contributed equally to this study.

1 | INTRODUCTION

Age-related macular degeneration (AMD) is characterized by changes in Bruch's membrane followed by dysfunction and atrophy of retinal pigment epithelial (RPE) cells.[1-3] The progression of the disease is multifactorial with both genetic and environmental components. Among these are oxidative and nitrosative stress associated with smoking, light exposure/phototoxicity, and impaired phagocytosis.[4-11] Epigenetic modifications have also been implicated in AMD pathophysiology.[12-16]

Aging causes morphological changes in Bruch's membrane, including calcification and fragmentation due to the sub-RPE deposits of drusen that are associated with macular degeneration.[3,17] Nonenzymatic nitrosylation due to smoking affects the properties of Bruch's membrane by cross-linking collagens in all layers of the structure.[8,10,18-20] In ex vivo culture systems that model AMD, abnormalities in the various layers of Bruch's membrane impair RPE cell reattachment, survival, and proliferation.[21-26] This implies an abnormal subretinal environment would hamper RPE transplantation.

The lack of adequate in vivo models for aging Bruch's membrane and atrophic AMD limits our understanding of the disease.[27,28] A variety of culture models have been devised. Several groups modeled the effects of age-related changes seen in early AMD, such as the development of sub-RPE deposits and drusen.[29-31] We devised a model for age-related changes to Bruch's membrane that is based on nonenzymatic nitration of extracellular matrix (ECM) that allows one to study RPE dysfunction in a compromised subretinal environment. The tissue culture method was validated ex vivo using aged or diseased Bruch's membrane.[19,32-35]

A new generation of culture models uses human-induced pluripotent stem cells (iPSCs) that are generated from adult somatic cells harvested from patients with AMD and other macular dystrophies.[29,36,37] These studies have shown that complement and inflammatory markers are upregulated in iPSC-derived RPE cells from patients with macular degenerations. Additionally, proteins that are overexpressed include components of drusen.

The current study combines our model for aging Bruch's membrane with iPSC-derived RPE cells from patients with AMD including geographic atrophy.

2 | METHODS

2.1 | Ethics statement

All experiments were conducted under the approval of the Yale University and Medical University of South Carolina Institutional Review Boards (IRB: 2000021266 and 2000020671, respectively) and after written, informed consent by study participants. This work was performed in adherence to the tenets of the Declaration of Helsinki.

Significance statement

Age-related macular degeneration (AMD) is a multifactorial disease of primates, which confounds efforts to model the disease in laboratory animals or in culture. The present culture model mimics aspects of the disease, as demonstrated by using stem cells derived from patients. The disease involves interactions between the retinal pigment epithelium, a layer of cells necessary for the function of photoreceptors, and the extracellular matrix upon which the epithelium sits. The differences observed between epithelia derived from normal and AMD patients were exacerbated when cells were cultured on a mimetic for diseased matrix. This model provides a robust platform for developing therapeutics.

2.2 | Primary fibroblast culture

Fibroblasts from AMD patients and patients with no history of AMD (Supplemental Table S1) were isolated as previously described.[32] Cultures were maintained in Dulbecco's Modified Eagle Medium (DMEM; Thermo Fisher Scientific, Waltham, Massachusetts, www.thermofisher.com) containing 10% fetal bovine serum (FBS; Thermo Fisher Scientific) and cultured in a humidified 37°C, 5% CO_2 incubator.

2.3 | Feeder free and nonintegration reprogramming method

Fibroblasts were grown to 5×10^4 cells/well and then treated with modified messenger ribonucleic acid (mRNA) encoding reprogramming factors, octamer-binding transcription factor 3,4 (Oct3/4), SRY (sex determining region Y)-box 2 (Sox2), Kruppel-like factor 4 (Klf4), c-Myc, NANOG homeobox protein (NANOG), and Lin-28 homolog A (Lin-28) using the fully automated platform New York Stem Cell Foundation (NYSCF) Research Institute Global Stem Cell Array as described previously[38] or using the Stemgent StemRNA 3rd Gen Reprogramming Kit (REPROCELL USA Inc., Beltsville, Maryland, www.reprocell.com) according to the manufacturer's protocol. iPSC cultures were expanded by passaging every 5-7 days using Accutase (Sigma-Aldrich, St. Louis, Missouri, www.sigmaaldrich.com) and cultured for use in downstream experiments.

2.4 | Immunofluorescence

Cells were fixed and stained as previously described.[32] A summary of antibodies used in this study is provided in the Supplemental

Material (Table S2). Cell nuclei were labeled with 4′,6-diamidino-2-phenylindole (DAPI; Sigma-Aldrich). Cells were visualized by a Zeiss LSM 800 confocal laser scanning microscope with the use of Zen microscope software (Carl Zeiss, Oberkochen, Germany, www.zeiss.com).

2.5 | Differentiation of human iPSCs into RPE cells

Human iPSC-derived RPE cell lines were differentiated as previously described.[32,39] Patches of pigmented iPSC-derived RPE cells were micro-dissected and plated onto laminin-coated plates until confluent. Cell cultures were then maintained in RPE cell differentiation medium and allowed to form monolayers. Cultures re-pigmented within 60-90 days.

2.6 | Transepithelial resistance (TER)

iPSC-derived RPE cells from donors were plated onto permeable membrane inserts (Corning Clear Transwell, 0.4 μm pore, 12 mm; Thermo Fisher Scientific). The cells were grown to confluence for at least 4 weeks in RPE differentiation medium containing 2% FBS. Barrier function of the iPSC-derived RPE cell monolayer was assessed by TER using an EVOM2 Epithelial Voltohmmeter with an STX2 electrode (World Precision Instruments, Sarasota, Florida, www.wpiinc.com). The resistance values for individual monolayers ($\Omega \times cm^2$) were determined from the average of four independent measurements and corrected for background resistance produced by a blank filter with culture medium.

2.7 | Phagocytosis assay

Bovine rod photoreceptor outer segments (ROS) were purchased from InVision BioResources company (Seattle, Washington, www.invisionbio.com), and fed to iPSC-derived RPE cells as previously described.[39] Ingested fluorescein isothiocyanate isomer I (FITC; ACROS Organics Thermo Fisher Scientific) labeled ROS were analyzed using a BioTek FLx800 plate reader (BioTek, Winooski, Vermont, www.biotek.com).

2.8 | Flow cytometry

Flow cytometry was performed at the Yale School of Medicine Cell Sorter Facility. FITC-labeled ROS were added to iPSC-derived RPE, unbound and cell membrane surface-bound ROS were removed by washing with Dulbecco's phosphate-buffered saline (DPBS; Thermo Fisher Scientific). The bound cells were treated with 0.25% trypsin containing 1 mM ethylenediaminetetraacetic acid (EDTA; Thermo Fisher Scientific), pelleted and washed with DPBS. Cells were then fixed with 4% formaldehyde solution (Thermo Fisher Scientific) in

DPBS and suspended in 1000 μL of DPBS with 2% FBS buffer. The samples were run on a LSRII flow cytometer (BD Biosciences, San Jose, California, www.bdbiosciences.com) and the data acquired with BD FACSDIVA software (BD Biosciences).

2.9 | Preparation of RPE cell-derived ECM and nitrite-modified ECM

RPE cell-derived ECM plates were prepared from ARPE-19 cells (used within five passages of obtaining them from the American Type Culture Collection (ATCC; Manassas, Virginia, www.atcc.org), as described previously.[26,32,35] ECM on 96-well plates were used to create two experimental plating surfaces (nontreated ECM and nitrite-modified ECM). Nitrite-modified ECM was prepared by adding 100 mM sodium nitrite to the ECM followed by incubation at 37°C for 7 days. Plates were then washed with DPBS and incubated with DPBS for 4 hours to completely remove the nitrite.

2.10 | Cell attachment assay

iPSC-derived RPE cells were plated on nontreated ECM or nitrite-modified ECM 96-well plates for 24 hours. Culture media were removed, and cells were washed once with DPBS before addition of Cell-Quant Cell Proliferation Assay reagents (GeneCopoeia, Rockville, Maryland, www.genecopoeia.com). The assay measures DNA content directly from culture wells. Cell attachment was determined by fluorescence signals acquired using a BioTek FLx800 plate reader (BioTek).

2.11 | Cell viability assay

iPSC-derived RPE cells were plated on nontreated ECM or nitrite-treated ECM 96-well plates for 24 hours. Cell viability was measured by RealTime-Glo MT Cell Viability Assay (Promega, Madison, Wisconsin, www.promega.com) according to the manufacturer's protocol. The assay measures the reducing potential of viable cells and is adenosine triphosphate (ATP)-independent. Luminescent signals were acquired using a BioTek FLx800 plate reader (BioTek).

2.12 | Measurement of mitochondrial function

Analysis of mitochondrial function was performed on live cells using the XFe96 Extracellular Flux Analyzer (Agilent Technologies, Santa Clara, California, www.agilent.com) and the Seahorse XF Cell Mito Stress Test (CMST) Kit (Agilent Technologies). To avoid differences due to unequal growth rates, iPSC-derived RPE cells were seeded onto a laminin-coated 96-well plate with a seeding density of 4×10^4 cell/well and grown until confluent. Data were normalized by cell

count. Cells were stained with DAPI and counted by ImageJ software (National Institute of Health, Bethesda, Maryland, www.nih.gov). Cells were then washed with CMST assay medium (XF base medium DMEM supplemented with 2 mM glutamine, 5.5 mM glucose, and 1 mM sodium pyruvate, pH 7.4; Agilent Technologies), followed by incubation for 1 hour at 37°C in a non-CO_2 incubator. Oxygen consumption rate was detected under basal conditions followed by the sequential addition of oligomycin, carbonyl cyanide 4-(trifluoromethoxy) phenylhydrazone (FCCP), rotenone, and antimycin A. From these sequential additions, the following parameters can be derived: basal respiration, ATP production, maximal respiration, and spare respiratory capacity.

2.13 | Microarray analysis

Microarray studies using Affymetrix GeneChip Human Clariom S arrays (Thermo Fisher Scientific) were performed at the Yale Center for Genomic Analysis (Yale University School of Medicine, New Haven, Connecticut). Total RNA was extracted from iPSC-derived RPE generated from five patients with a history of AMD and three patients with no history of AMD for downstream experiments. The Aurum Total RNA Mini Kit (Bio-Rad Laboratories, Hercules, California, www.bio-rad.com) was used according to the manufacturer's instructions. RNA quantity and quality were assessed by micro-volume spectrophotometry on the Nanodrop 2000 (Thermo Fisher Scientific) and by on-chip capillary electrophoresis on a Bioanalyzer 2100 (Agilent Technologies). Absorbance ratio at 260 and 280 nm was ≥1.9 and the RNA integrity number (RIN) was >9 for all samples. GeneChip WT Plus Reagent Kit (Thermo Fisher Scientific) was used for the preparation of samples and generation of ss-cDNA for hybridization. A 250 ng of total RNA was used for input. All reactions and hybridizations were carried out according to the manufacturer's protocol (Affymetrix; Thermo Fisher Scientific). Affymetrix GeneChip Human Clariom S arrays were washed using the GeneChip Fluidics Station 450 (Thermo Fisher Scientific) and scanned with the GeneChip Scanner 3000 (Thermo Fisher Scientific). Lines from each group (normal 1-3 and AMD 1-4 in Supplemental Table S1) were cultured separately. For microarray studies on nitrite-modified ECM, two normal and two AMD iPSC-derived RPE lines (normal 1 and 2; AMD 1 and 5 in Supplemental Table S1) were used in the analysis. Raw data were processed to perform gene-level normalization and quality control and analyzed using Affymetrix Expression Console Software (Thermo Fisher Scientific). Data deposited in the Gene Expression Omnibus (GEO) database (GSE125564). The table enumerates the $\log_2$ of the expression level. The fold change was calculated from the ratio of the expression levels of AMD vs normal samples. Negative values indicate that RPE from AMD express less than RPE derived from normal controls.

2.14 | Statistical analysis

Cell adhesion, viability, and mitochondrial functional assays were run using three normal and four AMD patient donor cells for three or more independent experiments. Data, statistical analysis, and graphing were performed using Prism ver. 8.1 (GraphPad Software, Inc., La Jolla, California, www.graphpad.com). We used the nonparametric Kruskal-Wallis test, followed by multi-comparison corrected Dunn's test. Graphs were generated to indicate the mean ± SE and a P value <.05 was considered statistically significant. Analysis of variance (ANOVA) empirical Bayes (eBayes) method adjusted statistical P values, which is suitable for small sample sizes, were used for calculation/analysis with Transcriptome Analysis Console (TAC; Thermo Fisher Scientific) for microarray studies. Expression level changes greater than 1.5-fold and adjusted P value <.05 are considered statistically significant.

3 | RESULTS

3.1 | Differentiation of human iPSCs into RPE cells

Reprogrammed iPSCs expressed OCT4, SOX2, stage-specific embryonic antigen 4 (SSEA-4), and keratin sulfate-associated antigens-1-60 (TRA-1-60) (provided as Supplemental Figure S1), indicating the pluripotency of these cells. As described in the Methods section, iPSCs from fibroblasts were induced to form embryoid bodies (EBs) (Figure 1A-C). Attached EBs then formed neural rosettes before RPE-like cells appeared in the culture (Figure 1D). At approximately 45 days, a hexagonal pigmented monolayer of RPE cells formed in culture (Figure 1E,F). These iPSC-derived RPE cells expressed RPE markers including the visual cycle protein retinal pigment epithelium-specific 65 kDa protein (RPE65), cellular retinaldehyde-binding protein (CRALBP), ezrin, and tight junction protein zonula occludens-1 (ZO-1) (Figure 1G).

An important function of RPE cells is the phagocytosis of ROS. Since iPSC-derived RPE cells expressed tyrosine-protein kinase Mer (MERTK),[40,41] which plays an important role in engulfing ROS, the ability of these cells to phagocytize ROS was explored. Phagocytized ROS particles localized within the cytoplasm of iPSC-derived RPE cells are shown in Figure 1H. Figure 1I,J represents the DAPI-labeled nuclei and merged image, respectively. An XZ projection demonstrates intracellular localization of FITC-labeled ROS (Figure 1K) in iPSC-derived RPE cells. At 24 hours, no significant difference in FITC percent intensity was seen between iPSC-derived RPE cells from AMD patients (108 ± 9%, 98 ± 11%, 104 ± 15%, 99 ± 11%) vs normal controls (100 ± 14%, 105 ± 6%, 99 ± 11%) (Figure 1L). These findings were corroborated using fluorescence activated cell sorting (provided as Supplemental Figure S3).

To further study the epithelial integrity and barrier function of patient-specific iPSC-derived RPE cell lines, we measured the TER. The TER in AMD patients (187 ± 6, 194 ± 7, 189 ± 4, and 198 ± 4 $\Omega \times cm^2$) vs the TER in normal controls (202 ± 5, 191 ± 7, and 197 ± 3 $\Omega \times cm^2$) revealed no significant difference (P > .05) (Figure 1M). These TER results are consistent with TER in other reported embryonic stem cell (ESC)-derived and iPSC-derived RPE cell lines.[29,40,41] Given the TER, high expression of claudin-3 and claudin-
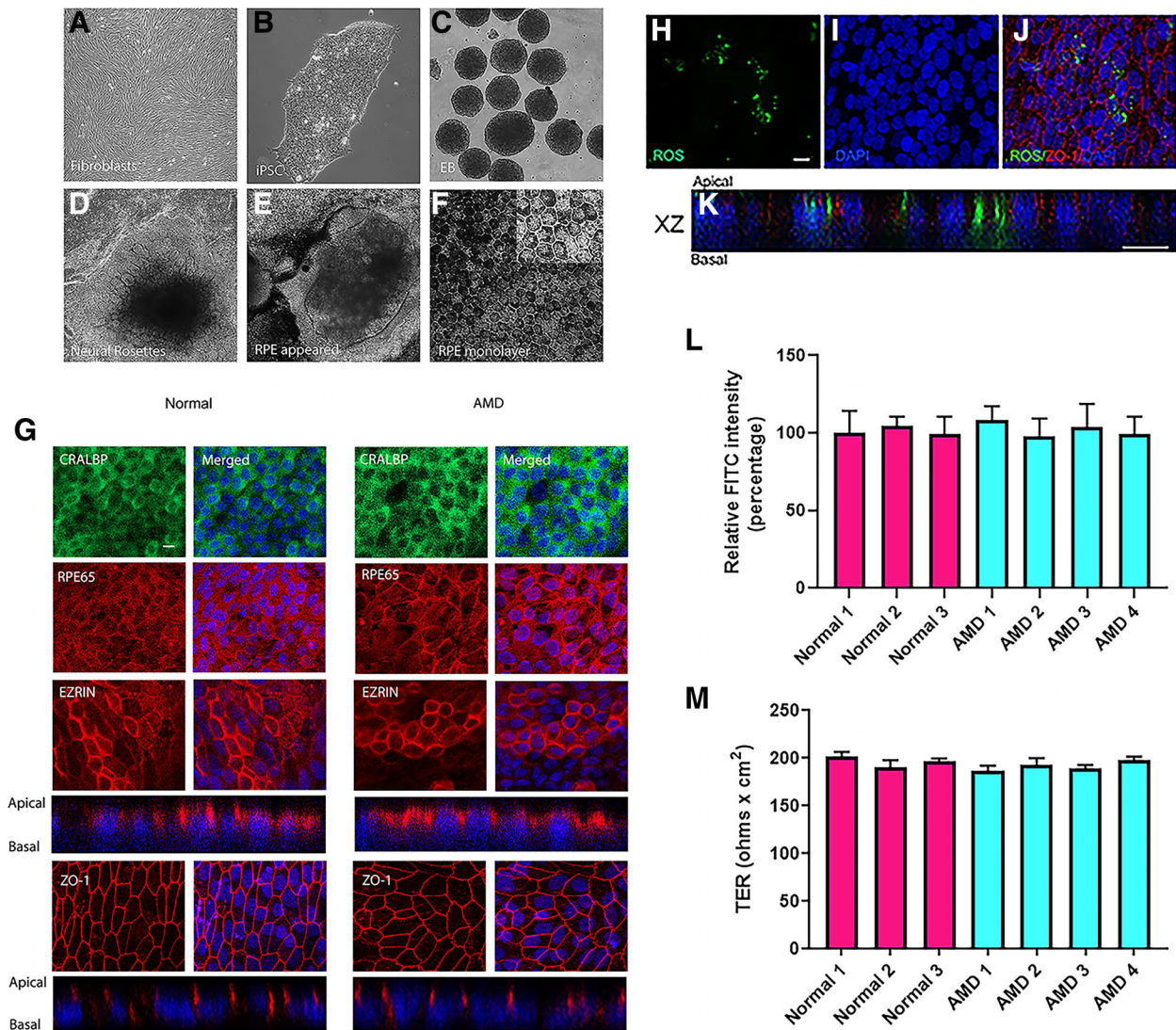
FIGURE 1 Differentiation of human-induced pluripotent stem cell (iPSC)-derived retinal pigment epithelial (RPE) cells from donor fibroblasts. Fibroblasts (A) were reprogrammed into an undifferentiated human iPSC colony (B). iPSCs were induced to become embryoid bodies (EBs) in a floating culture (C). Induction of neural rosettes by day 14 post-differentiation (D), and a pigmented monolayer of iPSC-derived RPE cells formed by day 45 post-differentiation (E, F). After differentiation, iPSC-derived RPE cell lines from age-related macular degeneration (AMD) and nondiseased donors (normal) stained positive for CRALBP, RPE65, ezrin, and ZO-1. Nuclei stained with DAPI (blue). Scale bar = 10 μm (G). The XZ projections demonstrate apical expression of ezrin (red) and apico-lateral expression of ZO-1 (red) in iPSC-derived RPE cells. FITC-labeled rod photoreceptor outer segments (ROS; green). Scale bar = 10 μm (H). Blue = DAPI staining (I). The merged-image demonstrate phagocytized ROS and ZO-1 expression in RPE cell cytoplasm (J). XZ projection shows intracellular localization of FITC-labeled ROS. Scale bar = 20 μm (K). ROS-FITC intensity was analyzed from AMD patients and normal controls at 24 hours (L). There were no significant differences among groups. These findings were corroborated using fluorescence activated cell sorting (Supplemental Figure S3). Monolayer integrity and permeability were assessed by transepithelial resistance (TER) in polarized iPSC-derived RPE cells. All seven iPSC-derived RPE cell lines show similar TER (M)

19 (Supplemental Table S3)[42,43] and circumferential bands of ZO-1, these iPSC-derived RPE cells from patient samples can establish barrier function in vitro. In addition, RPE marker genes were expressed and there was little difference in all six lines of iPSC-derived RPE cells (Supplemental Table S3).

These data confirm published studies that demonstrate the ability to establish RPE cell lines from patients with AMD and normal controls.[36,37] To determine if our cultures also demonstrated differences in the expression of diseased related proteins, we examined the entire transcriptome. There was little difference in the expression for most AMD, drusen-associated proteins, and inflammation/complement related transcripts. Nonetheless, the mRNAs for several of these genes were up-regulated in iPSC-derived RPE cells from AMD donors, including annexin A2, crystallin alpha-A (-B), and vitronectin (Table 1). The mRNAs for several genes were down-regulated in iPSC-derived RPE cells from AMD donors, including complement factor I (CFI), intracellular adhesion molecule 1 (ICAM-1), and TIMP metallopeptidase inhibitor 3 (TIMP3) (Table 1).

TABLE 1 AMD, drusen, and complement-related gene expression in normal and AMD iPSC-derived RPE cells

Categories (function)	Gene symbol	Gene name	Normal (log2)		AMD (log2)		AMD vs normal fold change	Adjusted P value
			Mean	SD	Mean	SD		
AMD and drusen associated genes	ANXA2	Annexin A2	14.96	0.12	15.93	0.4	1.96	.0034
	APOE	Apolipoprotein E	14.08	1.01	13.93	0.28	−1.11	.3147
	APP	amyloid beta (A4) precursor protein	16.23	0.51	15.81	0.05	−1.34	.1134
	CRYAA	Crystallin alpha A	11.85	3.16	17.43	0.51	47.55	.0201
	CRYAB	Crystallin alpha B	13.92	1.61	16.39	0.44	5.56	.0516
	TIMP3	TIMP metallopeptidase inhibitor 3	14.67	0.27	14.09	0.61	−1.5	.0164
	VEGFA	Vascular endothelial growth factor A	15.2	0.35	14.74	0.15	−1.38	.0518
	VTN	Vitronectin	5.89	1.09	7.94	0.65	4.12	.0401
Complement-related genes	ANG	Angiogenin, ribonuclease, RNase A family, 5	7.41	1.11	6.64	0.3	−1.71	.3552
	C1R	Complement component 1, r subcomponent	6.43	2.09	5.19	0.64	−2.37	.2568
	C1S	Complement component 1, s subcomponent	8.55	2.4	7.63	0.46	−1.89	.3525
	C3	Complement component 3	4.19	2.92	4.98	0.77	1.73	.4609
	C5	Complement component 5	6.16	0.12	6.01	0.27	−1.11	.4407
	CFH	Complement factor H	4.69	3.57	6.57	0.78	3.68	.9625
	CFI	Complement factor I	7.56	3.76	5.76	0.94	−3.49	.0454
	ICAM1	Intercellular adhesion molecule 1	8.77	0.83	7.66	0.18	−2.16	.0484

Note: Data derived from four patients with AMD (two atrophic; two exudative) and three individuals with no history of AMD.
Abbreviations: AMD, age-related macular degeneration; iPSC, induced pluripotent stem cell; RPE, retinal pigment epithelium.

3.2 | Nitrite modification of the ECM reduced attachment and cell viability of iPSC-derived RPE cells from patients with AMD

We previously demonstrated that nitrite-modification of the ECM affects the attachment and viability of primary or immortalized RPE cells.[26] We used this model of aged Bruch's membrane to test whether RPE derived from AMD patients was more susceptible than controls to the effects of nitrite-modified ECM. As documented below, iPSC-derived RPE cells from normal controls and AMD patients exhibited little difference with respect to cell attachment and survival on unmodified ECM (data provided as Supplemental Figure S2). Differences were observed on nitrite-modified ECM.

Compared to unmodified ECM, iPSC-derived RPE cells from normal controls were 11.75% (P < .01) less able to attach to nitrite-modified ECM (Figure 2A, individual RPE cell lines were combined and average). Compared to unmodified ECM, iPSC-derived RPE cells from AMD patients were 39.3% (P < .0001) less able to attach to nitrite-modified ECM (Figure 2A). A comparison of iPSC-derived RPE cells from normal controls vs AMD patients revealed that, cells from AMD patients were 27.6% (P < .01) less able to attach to nitrite-modified ECM (Figure 2A).

We then measured cell viability of these lines seeded on nitrite-modified ECM compared to nontreated ECM. Compared to unmodified ECM, the survival of iPSC-derived RPE from normal controls was reduced by 32.5% (P < .001) when cultured on nitrite-treated ECM (Figure 2B, individual RPE cell lines were combined and average). Compared to unmodified ECM, the survival of iPSC-derived RPE cells from AMD patents was reduced by 48.7% (P < .0001) when cultured on nitrite-treated ECM. A comparison of iPSC-derived RPE from normal controls vs AMD patients revealed that survival of cells from AMD patients was 15.1% (P > .05) lower on nitrite-modified ECM (Figure 2B). Although these results support previous observations that nitrite-modified ECM reduces RPE cell attachment and viability, the effect was heightened for RPE derived from patients with AMD.

3.3 | Differences in the expression of focal adhesion, proliferation, and energy-related genes underlie the effects revealed by nitrite-modified ECM

To look for potential mechanisms to explain the decreased attachment and viability of AMD iPSC-derived RPE, we examined the transcriptome of normal and AMD iPSC-derived RPE cells. Hierarchical clustering[44] revealed differences which clearly set apart the three normal iPSC-derived RPE cell lines from the four RPE cell lines derived from AMD patients (Figure 3). The results indicate that the gene
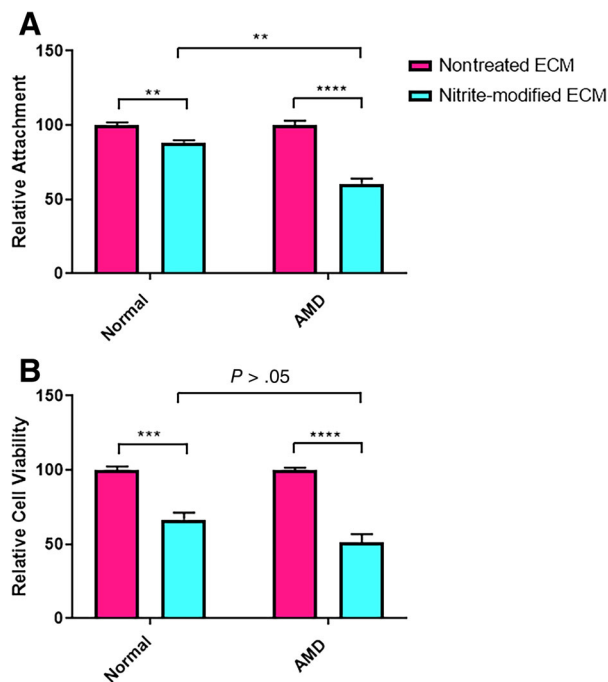
FIGURE 2 Reduced attachment and viability of induced pluripotent stem cell (iPSC)-derived retinal pigment epithelial (RPE) cells from age-related macular degeneration (AMD) patients compared with those of normal controls on nitrite-modified extracellular matrix (ECM). Cellular attachment was measured in four patients with AMD (two atrophic and two exudative) vs individuals with no history of AMD (normal, n = 3) on nitrite-modified ECM. Attachment was reduced in both RPE cells derived from AMD patients and normal controls. RPE cell attachment was reduced by 27.6% in RPE cells from AMD patients when compared to normal controls on nitrite-modified ECM (A). Cell viability was reduced in both RPE cells derived from four patients with AMD patients (two atrophic and two exudative) and individuals with no history of AMD (normal; n = 3 RPE cell lines) when seeded on nitrite-modified ECM (B). RPE cell viability was reduced by 15.1% in RPE cells from AMD patients when compared to normal controls on nitrite-modified ECM (B). **$P < .01$; ***$P < .001$; ****$P < .0001$

profiling of iPSC-derived RPE cells from AMD patients were different from normal controls. In RPE cells derived from AMD patients, altered gene expression patterns were related to metabolic and signal transduction pathways.[45] The mRNAs that were significantly lower in AMD samples included voltage-dependent calcium channel (CACNA1D), epidermal growth factor receptor (EGFR), fibroblast growth factor 14 (FGF14), forkhead box protein O1 (FOXO1), laminin alpha 5 subunit (LAMA5), and transient receptor potential cation channel subfamily V member 4 (TRPV4). In contrast, mRNAs that were higher in AMD samples included fibronectin 1 (FN1) and growth hormone receptor (GHR). These genes participate in the focal adhesion-PI3K-Akt-mTOR-signaling and energy/metabolic pathways (Table 2). This indicates that focal adhesion and metabolic functions may be altered in AMD iPSC-derived RPE. Accordingly, we compared mitochondrial respiration of iPSC-derived RPE from patients with AMD with normal controls.

3.3.1 | Decreased mitochondrial respiration and ATP production in iPSC-derived RPE cells from AMD patients

Our microarray array data showed altered gene expression in metabolic-related pathways (Table 2). Furthermore, earlier studies of bioenergetics demonstrate mitochondrial dysfunction in RPE cells from patients with AMD.[36,46] Therefore, we analyzed mitochondrial function of iPSC-derived RPE cells using the Seahorse platform.[47] We observed differences in metabolic capacity between AMD and normal RPE cell lines. Basal respiration (A), ATP production (B), maximal respiration (C), and spare respiratory capacity (D) were all significantly lower in all four AMD RPE cell lines, when compared to the three normal RPE cell lines (provided as Supplemental Table S4). The data are summarized in Figure 4.

3.4 | Nitrite modification of the ECM increased expression of complement pathway genes from patients with AMD compared to normal controls

To further investigate the phenotypic differences observed in RPE lines derived from patients with AMD compared to age-matched controls, we examined molecular alterations with regard to transcriptome profiling on cells cultured on nitrite-modified ECM. Based on our observations reported in Table 1 and previous reports,[29,37] we chose to investigate the expression of genes associated with the complement pathway given its relationship to a diseased matrix and the development of drusen.[48,49] Our analysis showed increased expression of several distinct complement pathway genes in RPE cells derived from patients with AMD vs age-matched controls cultured on nitrite-modified ECM. Complement-related genes upregulated in iPSC-derived RPE from AMD patients compared to age-matched controls were complement component 1, q subcomponent-like 1 (C1QL1), complement component 4B (C4B), complement component 4A (C4A), complement component 3 (C3), complement component 1, r subcomponent-like (C1RL), complement component 1, s subcomponent (C1S), complement component 1, r subcomponent (C1R), complement factor B (CFB), and complement factor H (CFH) (Figure 5). Additional information regarding complement-related gene is provided as Supplemental Table S5. These data together support a link between nonenzymatic nitration of ECM and upregulation of markers associated with disease pathology in AMD.

4 | DISCUSSION

Culture models relevant to human pathology can supplement the limitations of in vivo models.[50,51] The current study joins two others that studied RPE-related macular dystrophies by using patient-derived iPSC and age-matched controls. Saini et al[37] studied AMD including samples from donors with the age-related maculopathy susceptibility 2 (ARMS2)/HtrA serine peptidase 1 (HTRA1) homozygous genotype,
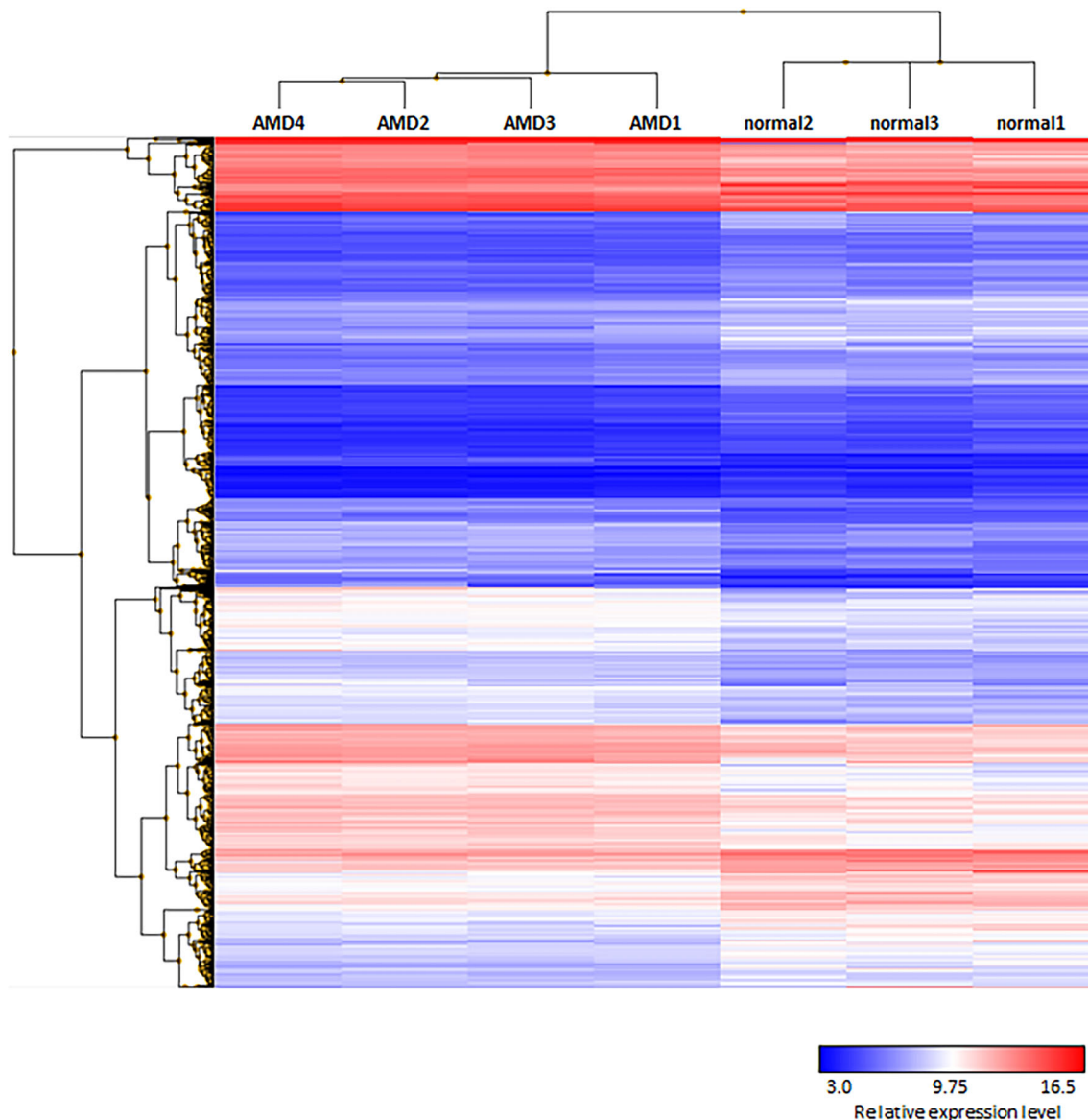
FIGURE 3 Transcriptome comparison of induced pluripotent stem cell (iPSC)-derived retinal pigment epithelial (RPE) cells. Hierarchical clustering revealed gene expression profiles of the four age-related macular degeneration (AMD) iPSC-derived RPE cell lines (two atrophic and two exudative) clustered together and revealed similar expression patterns while three control (normal) samples also clustered together

and Galloway et al[29] studied three slow retinal degenerations: Sorsby's fundus dystrophy, Doyne honeycomb retinal dystrophy/malattia leventinese, and autosomal dominant radial drusen. Although the number of patients used in each study was small, together they constituted an expanding database.

One concern for using iPSCs to study these diseases is that each develops over many years and iPSCs are young in that they have reverted into an embryonic-like state. Moreover, iPSC-derived RPE are differentiated over a course of months. In contrast, RPE in vivo is long-lived and accumulates insults not experienced by iPSC-derived RPE. These include a highly oxidative environment due to light exposure and the daily phagocytosis/degradation of shed photoreceptor disc membranes. Numerous studies demonstrate that stem cell-

derived RPE exhibit many RPE cell functions, but analysis of the transcriptome suggests they have not yet fully matured.[43]

At a superficial level, each study reported many similarities among RPE derived from patients and age-matched controls. The RPE exhibited epithelial morphology, functional tight junctions, and a TER >150 $\Omega \times cm^2$. The expression of RPE markers was similar at the mRNA and protein levels. Our study further demonstrated little difference in phagocytosis among RPE derived from patients and age-matched controls. Despite these similarities, each study found that RPE exhibited differences that reflected the disease from which it was isolated.

Despite differences in experimental approach, all three studies found that patient-derived RPE overexpressed mRNAs and proteins

TABLE 2 Focal adhesion, proliferation, and energy-related gene expression in AMD and normal individual iPSC-derived RPE cells

| Gene symbol	Gene name	Normal (log2) Mean	SD	AMD (log2) Mean	SD	AMD vs normal fold change	Adjusted P value	Pathway
CACNA1D	Calcium channel, voltage-dependent, L type, alpha 1D subunit	8.22	0.81	6.56	0.26	−3.15	.0013	Energy-related
FOXO1	Forkhead box protein O1	4.99	0.56	3.91	0.31	−2.12	.0032	Energy-related
EGFR	Epidermal growth factor receptor	8.76	1.31	8.16	0.37	−1.52	.0397	Focal adhesion
LAMA5	Laminin, alpha 5	9.79	0.39	7.75	0.64	−4.1	.0005	Focal adhesion
TRPV4	Transient receptor potential cation channel, subfamily V, member 4	5.33	0.67	4.34	0.26	−1.98	.0031	Focal adhesion
FGF14	Fibroblast growth factor 14	6.6	0.74	4.24	0.41	−5.14	.0009	Proliferation
FN1	Fibronectin 1	12.93	1.7	14.1	1.15	2.25	.0485	Proliferation
GHR	Growth hormone receptor	5.43	0.41	7.42	0.76	3.99	.0017	Proliferation

Note: Data derived from four patients with AMD (two atrophic; two exudative) and three individuals with no history of AMD.
Abbreviations: AMD, age-related macular degeneration; iPSC, induced pluripotent stem cell; RPE, retinal pigment epithelium.
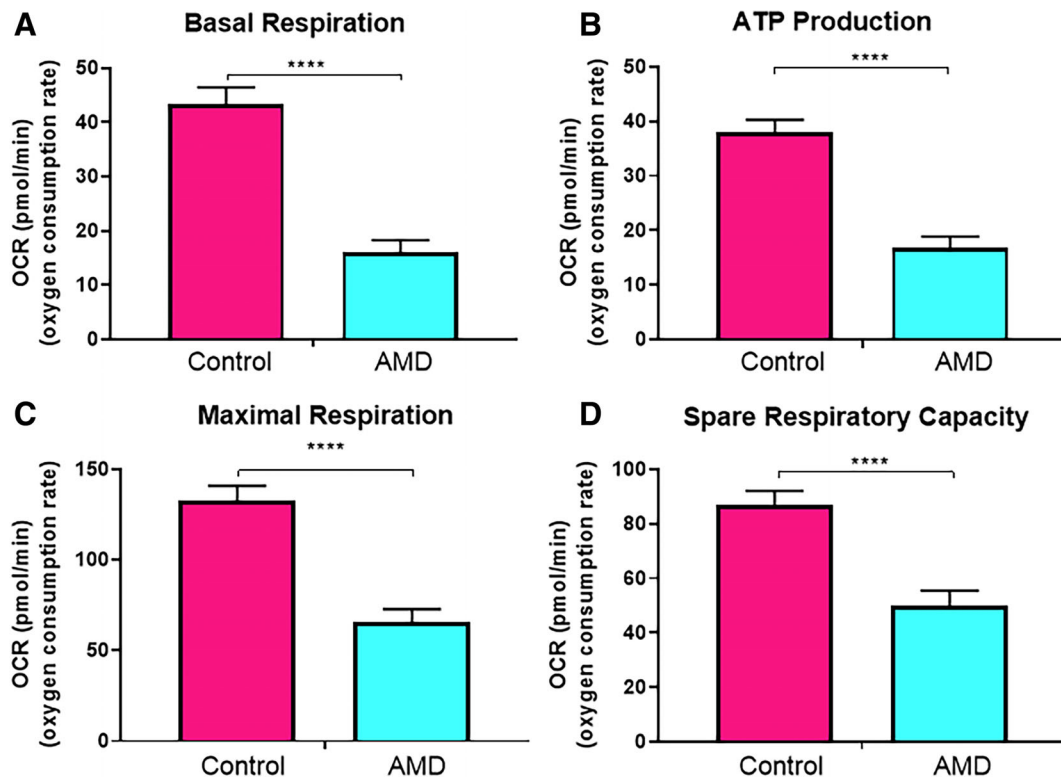
FIGURE 4 Measurement of mitochondrial function in induced pluripotent stem cell (iPSC)-derived retinal pigment epithelial (RPE) cells. Oxygen consumption rate (OCR) in RPE cells was measured by a Seahorse XF analyzer in 96-well plates to assess mitochondrial function by sequential addition of the following chemicals: Basal respiration (A), oligomycin to measure adenosine triphosphate (ATP) production (B) FCCP to measure maximal respiration (C), and a mix of rotenone and antimycin A to measure spare respiratory capacity (D). Basal respiration, ATP production, maximal respiration, and spare respiratory capacity were significantly reduced in RPE cell lines derived from four patients with age-related macular degeneration (AMD; two atrophic and two exudative), when compared with three RPE cell lines derived from individuals with no history of AMD (normal). All measurements were made with confluent cells, and all data were normalized by cell count. ****$P < .0001$

associated with the complement portion of the immune system. Complement has been implicated in these diseases and complement factors can induce the formation of drusen-like deposits in cultured

RPE.[30] Saini et al showed increased expression of mRNAs for apolipoprotein E (APOE), CFI, C1R, ICAM-1, and of C3 protein in some AMD lines, whereas cells cultured under normal conditions in our study
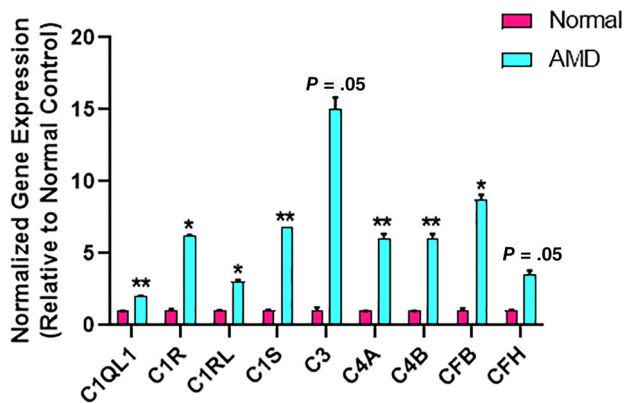
FIGURE 5 Increased expression of complement pathway genes in induced pluripotent stem cell (iPSC)-derived retinal pigment epithelial (RPE) cells cultured on nitrite-modified extracellular matrix (ECM). Analysis of gene expression with microarrays demonstrated increased expression of several complement pathway genes in iPSC-derived RPE cultures (n = 2 patients with atrophic age-related macular degeneration [AMD]) on nitrite-modified ECM compared with iPSC-derived RPE from age-matched controls (n = 2 individuals with no history of AMD). Complement-related genes upregulated in iPSC-derived RPE from AMD patients compared to age-matched controls were C1QL1, C4B, C4A, C3, C1RL, C1S, C1R, CFB, and CFH. Data are presented as mean + SE. *P < .05, **P < .01

revealed a decrease in mRNA. Additional to C1R and C3, Galloway et al[29] found increases in MCP, C1S, and C5. Furthermore, there were increases in drusen-like deposits with increased expression of APOE, TIMP3, and collagen IV. There was also an increase in crystallin alpha A/B (CRYAA and CRYAB). αA and αB crystallins belong to a family of heat shock proteins that have been detected in the RPE-Bruch's membrane-choroid complex of AMD patients. These proteins may serve to protect RPE cells from oxidative injury but may also play a role in the progression of angiogenesis in choroidal neovascularization.[52-54] Under basal conditions, our study demonstrated an increase in annexin A2 mRNA and a decrease in ICAM-1. The major finding in all of these studies is that the observed disease-related properties occurred within weeks or months, rather than the decades required in vivo.

To expand our survey, we examined the entire transcriptome using hierarchical clustering. Each AMD cell line clustered in a set that was distinct from that of the age-matched controls. The largest increase for the AMD lines was for CRYAA, a protein that also increased in the Galloway study.[29] Although this observation is intriguing, the biological significance of the high fold change in CRYAA in iPSC-derived RPE cells from AMD donors needs to be further explored.

Genes involved in energy/metabolism and signal transduction pathways were expressed in lower amounts in AMD-derived RPE. Moreover, RPE from AMD donors' mRNAs expressed higher levels of genes involved in the focal adhesion-PI3K-Akt-mTOR-signaling pathway, which was also observed in RPE cells directly isolated from AMD patients.[55] This pathway plays a critical role in cell-matrix adhesion, differentiation, and migration.[56-58] This pathway has also been implicated in the progression of age-related disease.[59] We previously

demonstrated the importance of ECM proteins such as laminin in RPE cell adhesion to Bruch's membrane.[21,33,60] We have also shown altered gene expression patterns in the aged retina,[61] and our data here may suggest that these patterns are exacerbated in the context of disease.

The effects on energy/metabolic pathways led us to analyze mitochondrial function. Consistent with previous reports, we found a decrease in metabolic capacity.[36,46] All four parameters (mitochondrial basal respiration, ATP production, maximal respiration, and spare respiratory capacity) were significantly lower in cell lines from individuals with AMD compared to normal controls. The reduced metabolic activity may point to why these diseased cells are less able to attach and proliferate on damaged ECM.

Conceivably, patient-derived RPE is more susceptible to stress, which might explain the results that have been discussed thus far for this and similar studies utilizing cells from AMD patients. Culture conditions are inherently imperfect and create their own stress. Monocultures of RPE lack interactions with the neural retina and choroid and grow on a stiff Transwell filter that has limited porosity.[62-64] Each of these elements may contribute to the formation of subepithelial deposits in normal cells, but the deposits of macular disease-derived RPE are qualitatively different. In the face of more physiologic stressors, these deposits become even more drusen-like.[29,30]

To explore the stressor hypothesis, we used an in vivo-like stressor that mimics an aspect of aging Bruch's membrane, nitrite-modified ECM. Seeding cells on this matrix revealed marked differences between normal and AMD-derived RPE. RPE derived from AMD patients were less able to attach and survive. Genes related to the complement system increased including C4B, C4A, C3, C1S, C1R, CFB, and CFH. Interestingly, C3a is formed by cleavage of C3 in the alternative complement pathway.[65] This is consistent with our previous data showing expression of C3a protein after culture on nitrite-modified ECM.[32] These findings indicate that lines derived from AMD patients display pathological phenotypes associated with AMD. Furthermore, nitrite-modified matrices serve as a relevant in vitro platform to study the RPE-ECM diseased interactions.

Our study adds to a growing literature that iPSCs generated from patients with macular diseases can mimic elements of the diseases, and that these elements are exacerbated by stress. The question becomes how patient-derived RPE express properties that require decades or a lifetime to develop in vivo. Conceivably, iPSC-derived RPE from patients retain some of the epigenetic markers acquired with aging, or their genetics may predispose them to be more sensitive to the ECM. Absent an environmental stressor, our AMD lines expressed few of the effects noted in the other two studies. The expression of genes could vary based on the stage or clinical classification of AMD.[66,67] Future studies with a larger sample size incorporating samples from patients with different stages of disease may reveal significant differences in the expression of these genes at baseline.

Although the current study did not examine subepithelial deposits, cells from AMD patients exhibited distinct differences in the transcriptome, physiologic function, and response to a mimetic for diseased Bruch's membrane. These factors should be considered when

transplanting a patient's iPSC-derived RPE into the stressful environment of a diseased Bruch's membrane with a degraded choroid and retina.

5 | CONCLUSION

In this study, we generated RPE from AMD patients and individuals with no history of AMD. No appreciable differences were seen among the RPE cell lines when performing functions such as phagocytosis of photoreceptor outer segments, and the ability to form tight junctions and barrier function. However, differences were seen between normal controls and AMD cohorts in gene profiling, metabolic function, and ability to survive on a model of aged Bruch's membrane. These findings indicate that aspects of pathology, such as the contribution of an altered sub-RPE environment, can be mimicked using RPE derived from patients with AMD and can serve as a relevant culture model to study disease. Furthermore, exploration of the critical differences among normal RPE and RPE from individuals with AMD should reveal mechanisms of disease and pave the way for novel therapeutic strategies.

CONFLICT OF INTEREST
The authors indicated no potential conflicts of interest.

AUTHOR CONTRIBUTIONS
J.G., H.C., and M.A.F.: collection and/or assembly of data; J.G., H.C., L.R., L.V.D.P., and M.A.F.: data analysis and interpretation; J.G., H.C., L.R., and M.A.F.: manuscript writing; NYSCF Global Stem Cell Array Team, S.N., and D.P.: provision of study materials; L.V.D.P. and M.A.F.: conception and design, financial support.

DATA AVAILABILITY STATEMENT
The data that support the findings of this study are openly available in in the NCBI Gene Expression Omnibus and are accessible through GEO Series accession number GSE125564.

ORCID
Mark A. Fields https://orcid.org/0000-0002-0185-0969

REFERENCES

1. Marshall GE, Konstas AG, Reid GG, Edwards JG, Lee WR. Type IV collagen and laminin in Bruch's membrane and basal linear deposit in the human macula. *Br J Ophthalmol*. 1992;76:607-614.

2. Pauleikhoff D, Harper CA, Marshall J, Bird AC. Aging changes in Bruch's membrane. A histochemical and morphologic study. *Ophthalmology*. 1990;97:171-178.

3. Booij JC, Baas DC, Beisekeeva J, Gorgels TG, Bergen AA. The dynamic nature of Bruch's membrane. *Prog Retin Eye Res*. 2010;29:1-18.

4. Tate DJ Jr, Miceli MV, Newsome DA. Phagocytosis and H_2O_2 induce catalase and metallothionein gene expression in human retinal pigment epithelial cells. *Invest Ophthalmol Vis Sci*. 1995;36:1271-1279.

5. Solberg Y, Rosner M, Belkin M. The association between cigarette smoking and ocular diseases. *Surv Ophthalmol*. 1998;42:535-547.

6. Borland C, Higenbottam T. Nitric oxide yields of contemporary UK, US and French cigarettes. *Int J Epidemiol*. 1987;16:31-34.

7. Beatty S, Koh H, Phil M, Henson D, Boulton M. The role of oxidative stress in the pathogenesis of age-related macular degeneration. *Surv Ophthalmol*. 2000;45:115-134.

8. Murdaugh LS, Wang Z, Del Priore LV, Dillon J, Gaillard ER. Age-related accumulation of 3-nitrotyrosine and nitro-A2E in human Bruch's membrane. *Exp Eye Res*. 2010;90:564-571.

9. Thao MT, Karumanchi DK, Yacout SM, Gaillard ER. Nitrite ion modifies tyrosine and lysine residues of extracellular matrix proteins. *Nitric Oxide*. 2018;79:51-56.

10. Wang Z, Paik DC, Dillon JP, Gaillard ER. Tyrosine nitration site specificity identified by LC/MS in nitrite-modified collagen type IV. *Exp Mol Med*. 2007;39:74-83.

11. Kunchithapautham K, Atkinson C, Rohrer B. Smoke-exposure causes endoplasmic reticulum stress and lipid accumulation in retinal pigment epithelium through oxidative stress and complement activation. *J Biol Chem*. 2014;289:14534-14546.

12. Blasiak J, Salminen A, Kaarniranta K. Potential of epigenetic mechanisms in AMD pathology. *Front Biosci (Schol Ed)*. 2013;5:412-425.

13. Wei L, Chen P, Lee JH, Nussenblatt RB. Genetic and epigenetic regulation in age-related macular degeneration. *Asia Pac J Ophthalmol*. 2013;2:269-274.

14. Porter LF, Saptarshi N, Fang Y, et al. Whole-genome methylation profiling of the retinal pigment epithelium of individuals with age-related macular degeneration reveals differential methylation of the SKI, GTF2H4, and TNXB genes. *Clin Epigenetics*. 2019;11:6.

15. Oliver VF, Jaffe AE, Song J, et al. Differential DNA methylation identified in the blood and retina of AMD patients. *Epigenetics*. 2015;10:698-707.

16. Nashine S, Nesburn AB, Kuppermann BD, Kenney MC. Age-related macular degeneration (AMD) mitochondria modulate epigenetic mechanisms in retinal pigment epithelial cells. *Exp Eye Res*. 2019;189:107701.

17. Spraul CW, Lang GE, Grossniklaus HE, Lang GK. Histologic and morphometric analysis of the choroid, Bruch's membrane, and retinal pigment epithelium in postmortem eyes with age-related macular degeneration and histologic examination of surgically excised choroidal neovascular membranes. *Surv Ophthalmol*. 1999;44(Suppl 1):S10-S32.

18. Bailey AJ, Paul RG, Knott L. Mechanisms of maturation and ageing of collagen. *Mech Ageing Dev*. 1998;106:1-56.

19. Paik DC, Dillon J, Galicia E, Tilson MD. The nitrite/collagen reaction: non-enzymatic nitration as a model system for age-related damage. *Connect Tissue Res*. 2001;42:111-122.

20. Chen L, Miyamura N, Ninomiya Y, Handa JT. Distribution of the collagen IV isoforms in human Bruch's membrane. *Br J Ophthalmol*. 2003;87:212-215.

21. Ho TC, Del Priore LV. Reattachment of cultured human retinal pigment epithelium to extracellular matrix and human Bruch's membrane. *Invest Ophthalmol Vis Sci*. 1997;38:1110-1118.

22. Tezel TH, Del Priore LV. Reattachment to a substrate prevents apoptosis of human retinal pigment epithelium. *Graefes Arch Clin Exp Ophthalmol*. 1997;235:41-47.

23. Del Priore LV, Tezel TH. Reattachment rate of human retinal pigment epithelium to layers of human Bruch's membrane. *Arch Ophthalmol*. 1998;116:335-341.

24. Zarbin MA. Analysis of retinal pigment epithelium integrin expression and adhesion to aged submacular human Bruch's membrane. *Trans Am Ophthalmol Soc*. 2003;101:499-520.

25. Gullapalli VK, Sugino IK, Van Patten Y, Shah S, Zarbin MA. Retinal pigment epithelium resurfacing of aged submacular human Bruch's membrane. *Trans Am Ophthalmol Soc*. 2004;102:123-137. discussion 137-128.

26. Wang Z, Paik DC, Del Priore LV, Burch RL, Gaillard ER. Nitrite-modified extracellular matrix proteins deleteriously affect retinal pigment epithelial cell function and viability: a comparison study with nonenzymatic glycation mechanisms. *Curr Eye Res*. 2005;30:691-702.

27. Nguyen HV, Li Y, Tsang SH. Patient-specific iPSC-derived RPE for modeling of retinal diseases. *J Clin Med*. 2015;4:567-578.

28. Zeiss CJ. Animals as models of age-related macular degeneration: an imperfect measure of the truth. *Vet Pathol*. 2010;47:396-413.

29. Galloway CA, Dalvi S, Hung SSC, et al. Drusen in patient-derived hiPSC-RPE models of macular dystrophies. *Proc Natl Acad Sci USA*. 2017;114:E8214-E8223.

30. Johnson LV, Forest DL, Banna CD, et al. Cell culture model that mimics drusen formation and triggers complement activation associated with age-related macular degeneration. *Proc Natl Acad Sci USA*. 2011;108:18277-18282.

31. Pilgrim MG, Lengyel I, Lanzirotti A, et al. Subretinal pigment epithelial deposition of drusen components including hydroxyapatite in a primary cell culture model. *Invest Ophthalmol Vis Sci*. 2017;58:708-719.

32. Fields MA, Bowrey HE, Gong J, Moreira EF, Cai H, Del Priore LV. Extracellular matrix nitration alters growth factor release and activates bioactive complement in human retinal pigment epithelial cells. *PLoS One*. 2017;12:e0177763.

33. Fields MA, Cai H, Bowrey HE, et al. Nitrite modification of extracellular matrix alters CD46 expression and VEGF release in human retinal pigment epithelium. *Invest Ophthalmol Vis Sci*. 2015;56:4231-4238.

34. Cai H, Gong J, Del Priore LV, Tezel TH, Fields MA. Culturing of retinal pigment epithelial cells on an ex vivo model of aged human Bruch's membrane. *JoVE*. 2018;134:e57084.

35. Moreira EF, Cai H, Tezel TH, Fields MA, Del Priore LV. Reengineering human Bruch's membrane increases rod outer segment phagocytosis by human retinal pigment epithelium. *Transl Vis Sci Technol*. 2015;4:10.

36. Golestaneh N, Chu Y, Cheng SK, Cao H, Poliakov E, Berinstein DM. Repressed SIRT1/PGC-1alpha pathway and mitochondrial disintegration in iPSC-derived RPE disease model of age-related macular degeneration. *J Transl Med*. 2016;14:344.

37. Saini JS, Corneo B, Miller JD, et al. Nicotinamide ameliorates disease phenotypes in a human iPSC model of age-related macular degeneration. *Cell Stem Cell*. 2017;20:635-647.e7.

38. Paull D, Sevilla A, Zhou H, et al. Automated, high-throughput derivation, characterization and differentiation of induced pluripotent stem cells. *Nat Methods*. 2015;12:885-892.

39. Gong J, Fields MA, Moreira EF, et al. Differentiation of human protein-induced pluripotent stem cells toward a retinal pigment epithelial cell fate. *PLoS One*. 2015;10:e0143272.

40. Hazim RA, Karumbayaram S, Jiang M, et al. Differentiation of RPE cells from integration-free iPS cells and their cell biological characterization. *Stem Cell Res Ther*. 2017;8:217.

41. Singh R, Phillips MJ, Kuai D, et al. Functional analysis of serially expanded human iPS cell-derived RPE cultures. *Invest Ophthalmol Vis Sci*. 2013;54:6767-6778.

42. Peng S, Gan G, Rao VS, Adelman RA, Rizzolo LJ. Effects of proinflammatory cytokines on the claudin-19 rich tight junctions of human retinal pigment epithelium. *Invest Ophthalmol Vis Sci*. 2012;53:5016-5028.

43. Peng S, Gan G, Qiu C, et al. Engineering a blood-retinal barrier with human embryonic stem cell-derived retinal pigment epithelium: transcriptome and functional analysis. *Stem Cells Translational Medicine*. 2013;2:534-544.

44. Aach J, Rindone W, Church GM. Systematic management and analysis of yeast gene expression data. *Genome Res*. 2000;10:431-445.

45. Slenter DN, Kutmon M, Hanspers K, et al. WikiPathways: a multifaceted pathway database bridging metabolomics to other omics research. *Nucleic Acids Res*. 2018;46:D661-D667.

46. Ferrington DA, Ebeling MC, Kapphahn RJ, et al. Altered bioenergetics and enhanced resistance to oxidative stress in human retinal pigment epithelial cells from donors with age-related macular degeneration. *Redox Biol*. 2017;13:255-265.

47. Pelgrom LR, van der Ham AJ, Everts B. Analysis of TLR-induced metabolic changes in dendritic cells using the seahorse XF(e)96 extracellular flux Analyzer. *Methods Mol Biol*. 2016;1390:273-285.

48. Fernandez-Godino R. Alterations in extracellular matrix/Bruch's membrane can cause the activation of the alternative complement pathway via tick-over. *Adv Exp Med Biol*. 2018;1074:29-35.

49. Fernandez-Godino R, Bujakowska KM, Pierce EA. Changes in extracellular matrix cause RPE cells to make basal deposits and activate the alternative complement pathway. *Hum Mol Genet*. 2018;27:147-159.

50. Tang S, Xie M, Cao N, Ding S. Patient-specific induced pluripotent stem cells for disease modeling and phenotypic drug discovery. *J Med Chem*. 2016;59:2-15.

51. Song MJ, Bharti K. Looking into the future: using induced pluripotent stem cells to build two and three dimensional ocular tissue for cell therapy and disease modeling. *Brain Res*. 2016;1638:2-14.

52. Kannan R, Sreekumar PG, Hinton DR. Alpha crystallins in the retinal pigment epithelium and implications for the pathogenesis and treatment of age-related macular degeneration. *Biochim Biophys Acta*. 2016;1860:258-268.

53. Nakata K, Crabb JW, Hollyfield JG. Crystallin distribution in Bruch's membrane-choroid complex from AMD and age-matched donor eyes. *Exp Eye Res*. 2005;80:821-826.

54. Kase S, He S, Sonoda S, et al. alphaB-crystallin regulation of angiogenesis by modulation of VEGF. *Blood*. 2010;115:3398-3406.

55. Newman AM, Gallo NB, Hancox LS, et al. Systems-level analysis of age-related macular degeneration reveals global biomarkers and phenotype-specific functional networks. *Genome Med*. 2012;4:16.

56. Comoglio PM, Boccaccio C, Trusolino L. Interactions between growth factor receptors and adhesion molecules: breaking the rules. *Curr Opin Cell Biol*. 2003;15:565-571.

57. Parsons JT. Focal adhesion kinase: the first ten years. *J Cell Sci*. 2003;116:1409-1416.

58. Petit V, Thiery JP. Focal adhesions: structure and dynamics. *Biol Cell*. 2000;92:477-494.

59. Zhao C, Vollrath D. mTOR pathway activation in age-related retinal disease. *Aging*. 2011;3:346-347.

60. Del Priore LV, Geng L, Tezel TH, Kaplan HJ. Extracellular matrix ligands promote RPE attachment to inner Bruch's membrane. *Curr Eye Res*. 2002;25:79-89.

61. Cai H, Fields MA, Hoshino R, Del Priore LV. Effects of aging and anatomic location on gene expression in human retina. *Frontiers Aging Neurosci*. 2012;4(8):1-20.

62. Benedicto I, Lehmann GL, Ginsberg M, et al. Concerted regulation of retinal pigment epithelium basement membrane and barrier function by angiocrine factors. *Nat Commun*. 2017;8:15374.

63. Ban Y, Rizzolo LJ. Differential regulation of tight junction permeability during development of the retinal pigment epithelium. *Am J Physiol Cell Physiol*. 2000;279:C744-C750.

64. Hotaling NA, Khristov V, Wan Q, et al. Nanofiber scaffold-based tissue-engineered retinal pigment epithelium to treat degenerative eye diseases. *J Ocul Pharmacol Ther*. 2016;32:272-285.

65. Ricklin D, Hajishengallis G, Yang K, Lambris JD. Complement: a key system for immune surveillance and homeostasis. *Nat Immunol*. 2010;11:785-797.

66. Ferris FL 3rd, Wilkinson CP, Bird A, et al. Clinical classification of age-related macular degeneration. *Ophthalmology*. 2013;120:844-851.

67. Mitchell P, Liew G, Gopinath B, Wong TY. Age-related macular degeneration. *Lancet*. 2018;392:1147-1159.

SUPPORTING INFORMATION

Additional supporting information may be found online in the Supporting Information section.